

**AEDC-TR-70-206**

DOC\_NUM SER CN  
UNC00752-PDC A 1



# **SOLENOIDS EXCITED AT RADIO-FREQUENCIES IN THE PRESENCE OF PLASMAS**

**J. A. Sprouse**

**ARO, Inc.**

**October 1970**

This document has been approved for public release and  
sale; its distribution is unlimited.

**ENGINE TEST FACILITY  
ARNOLD ENGINEERING DEVELOPMENT CENTER  
AIR FORCE SYSTEMS COMMAND  
ARNOLD AIR FORCE STATION, TENNESSEE**

**UNCLASSIFIED**

# ***NOTICES***

When U. S. Government drawings, specifications, or other data are used for any purpose other than a definitely related Government procurement operation, the Government thereby incurs no responsibility nor any obligation whatsoever, and the fact that the Government may have formulated, furnished, or in any way supplied the said drawings, specifications, or other data, is not to be regarded by implication or otherwise, or in any manner licensing the holder or any other person or corporation, or conveying any rights or permission to manufacture, use, or sell any patented invention that may in any way be related thereto.

Qualified users may obtain copies of this report from the Defense Documentation Center.

References to named commercial products in this report are not to be considered in any sense as an endorsement of the product by the United States Air Force or the Government.

**SOLENOIDS EXCITED AT RADIO-FREQUENCIES  
IN THE PRESENCE OF PLASMAS**

**J.A. Sprouse  
ARO, Inc.**

This document has been approved for public release and sale; its distribution is unlimited.

## FOREWORD

The work reported herein was sponsored by the Arnold Engineering Development Center (AEDC), Air Force Systems Command (AFSC), Arnold Air Force Station, Tennessee, under Program Element 62201F, Project 8952, Task 895207.

The research was conducted by ARO, Inc. (a subsidiary of Sverdrup & Parcel and Associates, Inc.), contract operator of AEDC, AFSC, under Contract F40600-71-C-0002. The work was conducted under ARO Project Nos. RW5010 and RW5011 in the Propulsion Research Area (R-2E-2) and (R-2G-1) of the Engine Test Facility (ETF) from September 1967 to December 1969, and the manuscript was submitted for publication as partial results of these research efforts on June 11, 1970.

The author wishes to acknowledge Dr. W.K. McGregor, Jr., and R.J. Bryson for suggestions which added materially to the work.

This technical report has been reviewed and is approved.

B. B. Algee  
Major, CF  
Research and Development  
Division  
Directorate of Technology

Harry L. Maynard  
Colonel, USAF  
Director of Technology

### ABSTRACT

The rf-excited coil in the presence of a plasma is examined in terms of a transformer model and also in terms of the distortion of the electromagnetic fields which is produced by the induced eddy-currents in the plasma. The treatment of rf coils presented here can be applied to either the plasma diagnostics regime or to the generation of the rf electrodeless discharge. Although the calculations of the electric and magnetic fields in this report are for a cylindrically symmetric coil immersed in a uniform, linear plasma, neither the model nor the approach to the problem is limited to these cases.

## CONTENTS

	<u>Page</u>
ABSTRACT . . . . .	iii
NOMENCLATURE . . . . .	v
I. INTRODUCTION . . . . .	1
II. TRANSFORMER MODEL . . . . .	2
III. ANALYTICAL PROCEDURES	
3.1 Figure of Merit $Q_s$ . . . . .	4
3.2 Azimuthal and Axial Electric Fields Associated with a Solenoid . . . . .	5
3.3 Calculation of Coil Parameters when the Plasma is External to the Solenoid . . . . .	6
3.4 Calculation of Coil Parameters when the Plasma is in the Interior of the Solenoid . . . . .	10
IV. CONCLUDING REMARKS . . . . .	13
REFERENCES . . . . .	13

## ILLUSTRATIONS

### Figure

1. Equivalent Circuit Model of an RF-Excited Coil in the Presence of a Plasma . . . . .	2
2. Two-Dimensional View of a Solenoid Immersed in a Plasma . . . . .	6
3. Experimental and Theoretical Data for the Figure of Merit $Q_s$ for a Solenoid Immersed in a Plasma . . . . .	9
4. Plot of $\Delta L/L$ and $\Delta R/R$ versus $x$ for a Solenoid Immersed in a Plasma . . . . .	9
5. Two-Dimensional View of Solenoid with a Plasma Core . . . . .	10
6. Experimental and Theoretical Data for the Figure of Merit $Q_s$ for Solenoid with a Plasma Core . . . . .	12

## APPENDIXES

I. PARALLEL-TUNED CIRCUIT AND MATCHING PROBLEMS . . . . .	17
II. SOLUTION TO MAXWELL'S EQUATIONS FOR A CYLINDRICALLY SYMMETRIC SYSTEM . . . . .	20

## NOMENCLATURE

a	Plasma radius
$\vec{B}$	Magnetic field vector
b	Coil radius
$\vec{E}$	Electric field vector

$I_p$	RMS current in the coil
$I_e$	RMS induced eddy-current in the plasma
$i_e(t)$	Instantaneous induced eddy-current in the plasma
$\hat{i}_\rho$	Unit radial vector
$\hat{i}_\phi$	Unit azimuthal vector
$\hat{i}_z$	Unit axial vector
$\vec{j}$	Current density
$j$	$\sqrt{-1}$
$k$	Coupling coefficient
$L$	Inductance of coil in free space
$L'$	Inductance of coil in a plasma
$L_e$	Equivalent inductance of the plasma
$\ell$	Axial length of the plasma
$\hat{n}$	Unit normal vector
$P_{coil}$	Power dissipated in the coil
$P_{in}$	Power input
$P_{plasma}$	Power dissipated in the plasma
$Q$	$\omega L/R$
$Q'$	$\omega L'/R'$
$Q_e$	$\omega L_e/R_e$
$R$	Internal resistance of the coil in free space
$R'$	Internal resistance of the coil in a plasma
$R_e$	Equivalent resistance of the plasma
$T$	Period of oscillation

$V$	Potential across the coil
$W_d$	Energy loss per cycle in the plasma
$\overline{W}_s$	Time-averaged energy stored in the electromagnetic fields produced by the eddy-currents
$x$	$a\sqrt{\omega\mu_0\sigma}$
$Z_{in}$	Input impedance of the coil
$a$	$(1-j)/\delta$
$\delta$	$(\omega\mu_0\sigma/2)^{-1/2}$ skin depth
$\epsilon$	Permittivity
$\mu$	Permeability
$\rho$	Radial coordinate
$\sigma$	Electrical conductivity
$\omega$	Angular frequency

#### Constants

$\epsilon_0$	$= 8.854 \times 10^{-12}$ farads/meter
$\mu_0$	$= 4\pi \times 10^{-7}$ henries/meter
$\pi$	$= 3.1416$



## SECTION I INTRODUCTION

Interest in the coupling between radio-frequency (rf) excited coils and conductive media stems from the fact that rf-excited coils are used both for generation of plasmas and for plasma diagnostics. In the diagnostic regime, rf coils have been used to measure plasma parameters such as electrical conductivity, gas flow velocity, and electron number density (Refs. 1, 2, and 3). RF induction heating of metals has long been a method of heat treating metals, and recently gas plasmas have been heated to high enthalpy levels using rf induction techniques (Refs. 4, 5, and 6). Although there is a gulf which separates these two areas of application of rf coils to plasma physics, there is a common denominator which links the two phenomena, namely, both are induced effects created by a time varying magnetic field. In the former case (i.e., plasma diagnostics), the fields are very weak, and the distortion of these fields by the presence of the plasma is related to various properties of the plasma. In the latter case, the fields are much stronger, and the coupling mechanism is much more involved since the conductivity of the plasma is not uniform. However, a great deal of useful insight can be obtained by treating the system as though it were uniform and isotropic.

Since, in the final analysis, it becomes necessary to explain the interaction between the coil and the plasma in terms of circuit phenomena (e.g., current, potential, resistance, inductance, and capacitance), it is expedient to employ from the beginning a model which characterizes the problem in terms of these quantities. It should be pointed out also that the model to be presented here does not require that the conductivity of the plasma be uniform. Rather, this requirement is used only to make some simple analytical calculations for illustrational purposes. A host of experimental evidence supports the use of a coupling model in which the plasma-coil relationship is approximated by a simple transformer circuit (Refs. 7, 8, and 9). In this model, the distribution of the induced eddy-currents is treated in terms of lumped circuit parameters which can be reflected into the primary circuit using ordinary transformer techniques. Hence, a qualitative analysis of the changes in the coil inductance and resistance in the presence of the plasma can be made. Exact values of the coil parameters in the presence of a plasma is obtained by solution of Maxwell's equation. In some simple geometrical configuration and for uniform conductivity or for some special cases (e.g., parabolic conductivity, Ref. 6), analytical expressions for these configurations are readily obtainable, whereas in the more complex cases, a numerical solution must be obtained.

Although the solution to the coupling problem must be sought by examining the induced eddy-currents, regardless of any particular model, the method in which this problem is treated can be simplified by seeking a correlating parameter which can be readily interpreted in terms of either circuit phenomena or field phenomena. The "figure of merit" or  $Q$  of a circuit (defined as the ratio of average energy stored to the energy loss per cycle) is a nondimensional parameter which is ideal for characterizing the eddy-currents, and it is also a parameter which is directly applicable to explaining circuit phenomena. The coupling between rf-excited coils and conductive media is explained in this report by exploiting the features associated with the figure of merit of the system ( $Q_s$ ) in conjunction with a simple transformer model. A comparison between theory and

experiment for solenoids immersed in conductive media indicates that the coupling can be accurately explained (both qualitatively and quantitatively) using the transformer model.

It should be noted that the analytical and experimental results presented in this report do not depend on the transformer model. This model is intended primarily for clarification and understanding. Similarly, the transformer model is not restricted to the simple case to be studied here.

## SECTION II TRANSFORMER MODEL

It has been observed that, when a nonmagnetic conductor is placed in the neighborhood of an rf-excited inductor, (1) eddy-currents are induced in the conductor, (2) the self inductance of the inductor decreases, and (3) the internal resistance associated with the inductor increases. These effects are also produced when a closed secondary circuit is inductively coupled to the inductor. This parallelism suggests a simple model which can be used to (qualitatively) explain the coupling mechanism between rf coils and conductive media (plasmas). That is, the eddy-currents may be treated by lumping the distributed inductance and resistance associated with each closed current path into a total equivalent inductance ( $L_s$ ) and total equivalent resistance ( $R_s$ ). Further, if it is assumed that the coil is inductively coupled to the plasma through a coupling coefficient  $k$ , then the effects caused by the presence of the plasma can be easily examined by reflecting the lumped inductance and resistance into the coil using ordinary transformer analysis. This procedure is schematically illustrated in Fig. 1.

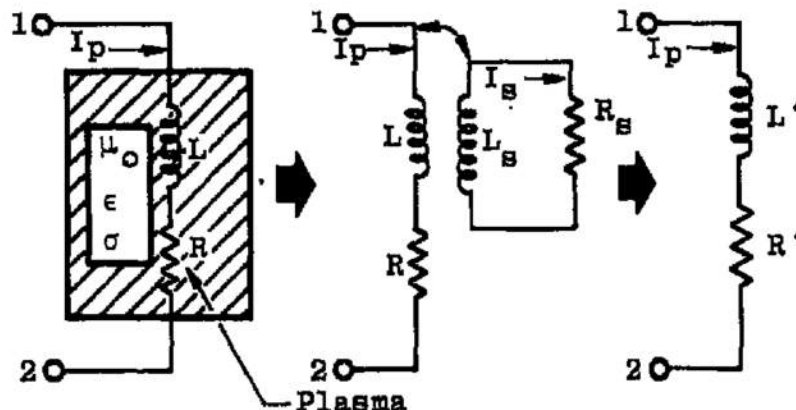


Fig. 1 Equivalent Circuit Model of an RF-Excited Coil in the Presence of a Plasma

From this figure, it can be seen that the process is divided into three successive steps. First, the coil with free-space inductance  $L$  and resistance  $R$  is shown immersed in

a conductive medium. In the second step, the inductance and resistance associated with the induced eddy-currents are treated as a closed secondary circuit coupled to the primary circuit through a coupling coefficient  $k$ . In the third step, the secondary circuit is reflected into the primary circuit which results in a new coil whose inductance and resistance ( $L'$  and  $R'$ ) can be obtained directly from the loop equations for the circuit shown in the center of Fig. 1. That is,

$$V = (R + j\omega L) I_p + (j\omega k\sqrt{LL_s}) I_s \quad (1)$$

$$0 = (j\omega k\sqrt{LL_s}) I_p + (R_s + j\omega L_s) I_s \quad (2)$$

where  $V$  is the applied potential across points (1) and (2) in Fig. 1, or rearranging Eq. (2) gives

$$I_s = \left( \frac{-j\omega k\sqrt{LL_s}}{R_s + j\omega L_s} \right) I_p \quad (3)$$

Substituting for  $I_s$  in Eq. (3) and taking the ratio  $V/I_p$  yield the input impedance  $Z_{in}$  of the coil:

$$Z_{in} = \frac{V}{I_p} = R \left[ 1 + \frac{k^2(\omega L)(\omega L_s) R_s}{R[R_s^2 + (\omega L_s)^2]} \right] + j\omega L \left[ 1 - \frac{k^2(\omega L_s)^2}{R_s^2 + (\omega L_s)^2} \right] \quad (4)$$

Equation (4) can be written in the form

$$Z_{in} = R' + j\omega L' \quad (5)$$

where

$$L' = L \left[ 1 - \frac{k^2(\omega L_s)^2}{R_s^2 + (\omega L_s)^2} \right] \quad (6)$$

and

$$R' = R \left[ 1 + \frac{k^2(\omega L)(\omega L_s) R_s}{R[R_s^2 + (\omega L_s)^2]} \right] \quad (7)$$

If the nondimensional parameters  $Q = \omega L/R$ ,  $Q' = \omega L'/R'$ , and  $Q_s = \omega L_s/R_s$  are substituted into Eqs. (6) and (7), then the following useful relationships are obtained:

$$\frac{L'}{L} = \frac{1 + Q_s^2(1 - k^2)}{1 + Q_s^2} \leq 1 \quad (8)$$

$$\frac{R'}{R} = \frac{Q_s^2 + k^2 Q Q_s + 1}{Q_s^2 + 1} \geq 1 \quad (9)$$

and

$$\frac{Q'}{Q} = \frac{1 + Q_p^2(1 - k^2)}{Q_p^2 + k^2 Q Q_p + 1} \leq 1 \quad (10)$$

The figure of merit  $Q_p$ , which is associated with the induced eddy-currents in the plasma can be expressed in terms of the measurable quantities  $L$ ,  $L'$ ,  $R$ , and  $R'$  by eliminating the coupling coefficient  $k$  in Eqs. (8) and (9). That is,

$$Q_p = \frac{\omega L_p}{R_p} = \frac{\omega(L - L')}{R' - R} = \omega \left( \frac{\Delta L}{\Delta R} \right) \quad (11)$$

The average power input into the plasma-coil system can be expressed in terms of  $L$ ,  $Q$ ,  $Q_p$ ,  $k$ , and the current  $I_p$ :

$$P_{in} = P_{coil} + P_{plasma} = I_p^2 R' \quad (12)$$

where

$$P_{coil} = I_p^2 \left( \frac{\omega L}{Q} \right) \quad (13)$$

and

$$P_{plasma} = I_p^2 R_p = I_p^2 \left( \frac{\omega L}{Q} \right) \left( \frac{k^2 Q Q_p}{Q_p^2 + 1} \right) = \left( \frac{k^2 Q Q_p}{Q_p^2 + 1} \right) P_{coil} \quad (14)$$

A number of conclusions regarding the application of rf-excited coils to specific problem areas can be made from examination of Eq. (14). For example, it can be seen that, for diagnostic applications, it is necessary that  $P_{coil}$  be small (of the order microwatts) so that the plasma is undisturbed, while for rf plasma generation, it is desirable to have  $P_{plasma} \gg P_{coil}$  (i.e.,  $Q_p = 1$  and  $k^2 Q \gg 1$ ) and  $P_{plasma}$  to be of the order of kilo- to megawatts. In addition to these considerations, it is also important to consider matching between the coil and electronics as well as matching between the coil and the plasma. A brief discussion of this matching is presented in Appendix I.

### SECTION III ANALYTICAL PROCEDURES

#### 3.1 FIGURE OF MERIT $Q_p$

The emphasis to this point has been to describe the coupling between the coil and plasma in terms of circuit parameters. This is useful because, in the final analysis, measurements of the system are greatly simplified if everything can be put in terms of linear circuit elements. However, while this approach is desirable in establishing methods of measuring electrical conductivity or in measuring such things as the input power to rf-generated plasmas, it does not lead to a direct relationship between the measured quantities (e.g.,  $I_p$ ,  $Q'$ ,  $L'$ , or  $R'$ ) and the electrical properties of the plasma (e.g.,  $\sigma$ ,  $\mu$ ,  $\epsilon$ ,

etc.). This portion of the report will be concerned with calculating the coil parameters in terms of the geometry and plasma properties. First, a cylindrical coil will be treated in which the plasma is external to the solenoid. Then, the same analysis will be applied where the plasma is in the interior of the coil.

The relationship between circuit phenomena and field phenomena can be established by expressing  $Q_s$  in terms of the electromagnetic fields generated by the eddy-currents. The defining equation is

$$Q_s = 4\pi \frac{\bar{W}_s}{W_d} = 4\pi \left[ \frac{\text{Time averaged energy stored}}{\text{Energy loss per cycle}} \right] = 4\pi \left[ \frac{\frac{1}{2} L_s I_s^2}{\frac{2\pi}{\omega} R_s I_s^2} \right] \quad (15)$$

### 3.2 AZIMUTHAL AND AXIAL ELECTRIC FIELDS ASSOCIATED WITH A SOLENOID

The energy stored and energy loss per cycle can be calculated when the electric and magnetic fields are known throughout the volume of interest. In fact, complete knowledge of the electric and magnetic fields is sufficient to determine all electric and magnetic phenomena which may occur within this volume of interest. The following sections will be concerned with calculating these fields from Maxwell's equations for certain prescribed conditions. Obviously, some major simplifications and limitations are necessary to obtain closed-form solutions to Maxwell's equations for these particular cases. For the main part, these simplifications and limitations are noted during the calculations. However, there is one subtle simplification which requires additional consideration although the introduction of this simplification does not alter the calculations in this report. In the calculations throughout this report, it is assumed that the electric field is derivable from only a time-varying magnetic field (induction). (That is, it is assumed that  $\nabla \cdot \mathbf{E} = 0$ .) Although this is generally true for the field space, it does not apply to the surface of the coil since there are time-varying charges along the coil which give rise to an electric field (potential). This field has principally an axial component, which is often eliminated by constructing a Faraday cage<sup>1</sup> about the coil. Since the source impedance of this electric field is quite large, these fields cannot deliver appreciable power into a highly conducting medium because they are effectively "shorted-out" by the presence of a good conductor. This is precisely why a Faraday cage can be successfully used to eliminate the axial electric field, and also explains how they are eliminated in a high-power (sometimes referred to as "inductive") rf discharge without the addition of a Faraday cage. On the other hand, the azimuthal field is associated with a system which has a low source impedance, and any attempt to "short" these fields leads ultimately to rf induction heating since it is possible to deliver large amounts of power from the load coil to the conductor in this mode of operation. In rf plasma discharges, the discharge which is the result of the axial electric field is often referred to as "low-power," "capacitive," or "E-field" discharge, whereas the discharge which is the result of the azimuthal electric field is referred to as "high-power,"

<sup>1</sup>A Faraday cage can be built by placing conducting wires around or inside a coil such that they are in alignment with the axial electric field but arranged such that they do not interfere with the azimuthal induction electric field.

"inductive," or "H-field" discharge. The remainder of this report will be concerned only with the "induced electric" field since the axial electric field can either be eliminated or neglected.

### 3.3 CALCULATION OF COIL PARAMETERS WHEN THE PLASMA IS EXTERNAL TO THE SOLENOID

To express  $Q_s$  in terms of the stored energy and energy loss, the electromagnetic fields associated with the induced eddy-currents must be calculated from Maxwell's

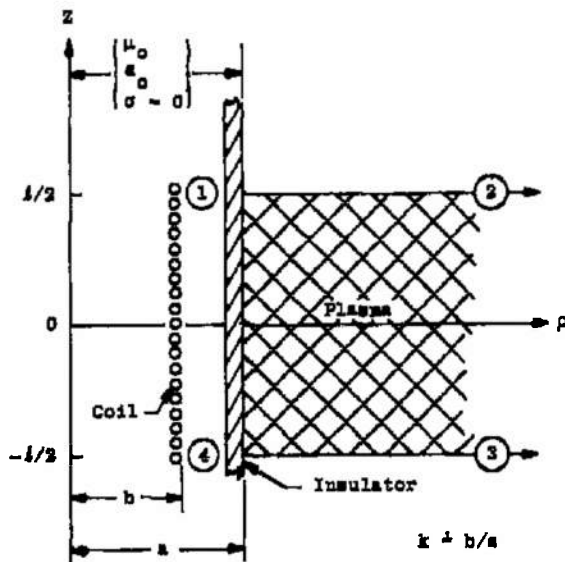


Fig. 2 Two-Dimensional View of a Solenoid Immersed in a Plasma

equations. While it is impossible to obtain a closed-form solution for a general current distribution, there are certain geometric configurations in which the symmetry allows some major simplifications. In particular, when an rf coil, whose length is large compared with its diameter, is immersed in a uniform plasma as shown in Fig. 2, then the following statements are useful in simplifying the problem: (1) the induced eddy-currents have only an azimuthal component, (2) the magnetic field produced by the eddy-currents in the free space region ( $0 \leq \rho$ ) is uniform, and (3) the electric and magnetic fields in the plasma vary predominantly in the radial coordinate; thus all derivatives in the other coordinates may be neglected.

Since the magnetic field produced by the eddy-currents in the region ( $0 \leq \rho \leq a$ ) is assumed to be constant, then the time-averaged energy stored can be calculated quite simply. That is,

$$\bar{W}_s = \frac{1}{T} \int_0^T \left[ \frac{1}{2} \int_{-l/2}^{l/2} \int_0^{2\pi} \int_0^a \left( \frac{\vec{B} \cdot \vec{B}}{\mu_0} + \epsilon \vec{E} \cdot \vec{E} \right) \rho d\rho d\phi dz \right] = \frac{\pi a^2 l B_s^2}{4\mu_0} \quad (16)$$

where  $B_s$  is the magnetic field at the boundary which is produced by the eddy currents, and  $T = 2\pi/\omega$  is the period of oscillation. (MKS units will be used exclusively in this report.)

To illustrate that this expression for  $\bar{W}_s$  is consistent with the circuit interpretation of  $\bar{W}_s$ , the integral form of Ampere's law can be used to obtain the relationship between the secondary current  $I_s$  (see Fig. 1) and the magnetic field. Ampere's law is

$$\oint_C \vec{B} \cdot d\vec{\ell} = \int \int \vec{J} \cdot \hat{n} da = \mu_0 i_s(t) \quad (17)$$

If the path of integration  $C$  is around the loop as indicated by the points 1, 2, 3, 4, 1, in Fig. 2, then

$$\oint_{1,2,3,4,1} \vec{B} \cdot d\vec{\ell} = \ell B_a = \mu_0 i_s(t) \quad (18)$$

Equation (18) can be written in terms of the rms current  $I_s$ ; that is,

$$I_s = \frac{\ell B_a}{\sqrt{2} \mu_0} \quad (19)$$

Thus, the expression for the time average of the stored energy  $\overline{W}_s$  becomes

$$\overline{W}_s = \frac{\pi a^2 \ell B_a^2}{4\mu_0} = \frac{1}{2} \left( \frac{\pi a^2 \mu_0}{\ell} \right) I_s^2 = \frac{1}{2} L_s I_s^2 \quad (20)$$

where

$$L_s = \frac{\pi a^2 \mu_0}{\ell} \quad (21)$$

From this expression, it is evident that the equivalent inductance associated with the induced eddy-currents in the plasma is to a first approximation determined by the geometry of the system and is independent of the conductivity of the plasma. Thus, from this analysis, it is seen that the equivalent inductance of the plasma  $L_s$  behaves quite like that of ordinary inductors.

To obtain the energy loss per cycle, the fields in the region ( $\rho \geq a$ ) must be obtained from Maxwell's equations. The equations can be simplified by making use of the fact that the spatial variation of the fields normal to the conductive surface is much more rapid than variations parallel to the surface; hence, all derivatives with respect to coordinates parallel to the surface can be neglected as compared with the normal derivatives. Thus, the gradient operator  $\vec{\nabla}$  may be replaced by (Ref. 10):

$$\vec{\nabla} = \hat{i}_\rho \frac{\partial}{\partial \rho} \quad (22)$$

Therefore, Maxwell's equations for the fields in the plasma can be written as

$$\hat{i}_\rho \times \frac{\partial \vec{B}_c}{\partial \rho} = u_0 \sigma \vec{E}_c \quad (23)$$

and

$$\hat{i}_\rho \times \frac{\partial \vec{E}_c}{\partial \rho} = -j\omega \vec{B}_c \quad (24)$$

In addition to the assumptions listed above, it has been implicitly assumed that (1) the time variance of the fields is sinusoidal (i.e.,  $e^{j\omega t}$ ), (2) the eddy-current  $\vec{J}_c$  is related to the electric field  $\vec{E}_c$  according to Ohm's law (i.e.,  $\vec{J}_c = \sigma \vec{E}_c$ ), and (3) the displacement current in the conductive media can be neglected (i.e.,  $\sigma \gg \omega \epsilon$ ).

The magnetic and electric fields in the plasma which satisfy Eqs. (23) and (24) along with the boundary conditions  $B_c = B_a$  at  $\rho = a$  are

$$\vec{B}_c = \hat{i}_z B_a \exp [-\alpha (\rho - a)] \quad (25)$$

and

$$E_c = -\hat{i}_\phi \frac{B_a \omega \alpha \delta^2}{2} \exp [-\alpha (\rho - a)] \quad (26)$$

where

$$\alpha = (1 - j)/\delta$$

and

$$\delta = (2/\omega\mu_0\sigma)^{1/2} = \text{"skin-depth"}$$

The energy dissipated per cycle  $W_d$  is

$$W_d = \left(\frac{2\pi}{\omega}\right) \frac{1}{2} \int_{-l/2}^{l/2} \int_0^{2\pi} \int_a^\infty \sigma E_c \cdot E_c^* \rho d\rho d\phi dz \quad (27)$$

Substituting for  $E_c$  in Eq. (27) yields

$$W_d = \frac{\pi^2 l B_a^2}{2\mu_0} \left[ \delta^2 \left( 1 + \frac{2a}{\delta} \right) \right] = \left( \frac{2\pi}{\omega} \right) I_a^2 R_s \quad (28)$$

If Eq. (19) is substituted into Eq. (28) and then solved for  $R_s$ , the following expression for  $R_s$  is obtained:

$$R_s = \frac{2\pi (a + \delta/2)}{\sigma l \delta} \quad (29)$$

From this equation, it is noted that the equivalent resistance associated with the induced currents in the plasma is simply the same resistance that is observed for a uniform conductor whose cross-sectional area is  $l\delta$  and conductance length is  $2\pi(a + \delta/2)$ .

The figure of merit  $Q_s$  for the cylindrically symmetric system shown in Fig. 2 is obtained by substituting Eqs. (20) and (28) into Eq. (15). That is,

$$Q_s = 2 \left[ \frac{a^2/\delta^2}{1 + 2a/\delta} \right] = \frac{x^2}{1 + \sqrt{2} x} \quad (30)$$

where

$$x = \sqrt{2} a/\delta = a\sqrt{\omega\mu_0\sigma}$$

Equation (30) is plotted in Fig. 3 versus the nondimensional parameter  $x$ . This figure also contains some experimental data which were obtained using a number of different cylindrical coils immersed in various conductors whose conductivities extended from 10



mhos/m (electrolytic solutions) to  $10^6$  mhos/m (mercury). The coil inductance and coil Q were measured with a Q-meter when the coil was immersed in these conductors while the frequency was varied between 2 and 20 mHz. This measurement process is outlined in detail in Ref. 7. A comparison between theory and experiment indicates that the transformer model adequately describes (both qualitatively and quantitatively) rf coils immersed in conductive media over a wide range of conductivities and frequencies.

Since rf coils are normally the complementary part of a tuned circuit whose function in the electrical network may be either frequency controlled and/or matching, it is important to be aware of how the coil behaves with various plasma conditions. This can be accomplished by examining the changes in coil inductance  $\Delta L$  and coil resistance  $\Delta R$  in terms of  $x$ . Thus, if Eq. (30) is substituted into Eqs. (8) and (9), then the following equations for  $\Delta L$  and  $\Delta R$  as a function of  $x$  are obtained:

$$\frac{\Delta L}{L} = \frac{L - L'}{L} = k^2 \left[ \frac{x^4}{x^4 + 2x^2 + 2\sqrt{2}x + 1} \right] \quad (31)$$

and

$$\frac{\Delta R}{R} = \frac{R' - R}{R} = k^2 Q \left[ \frac{x^2(1 + \sqrt{2}x)}{x^4 + 2x^2 + 2\sqrt{2}x + 1} \right] \quad (32)$$

These ratios are plotted in Fig. 4. From this figure, it can be seen that the change in coil inductance is small for small values of conductivity and increases to a saturation value

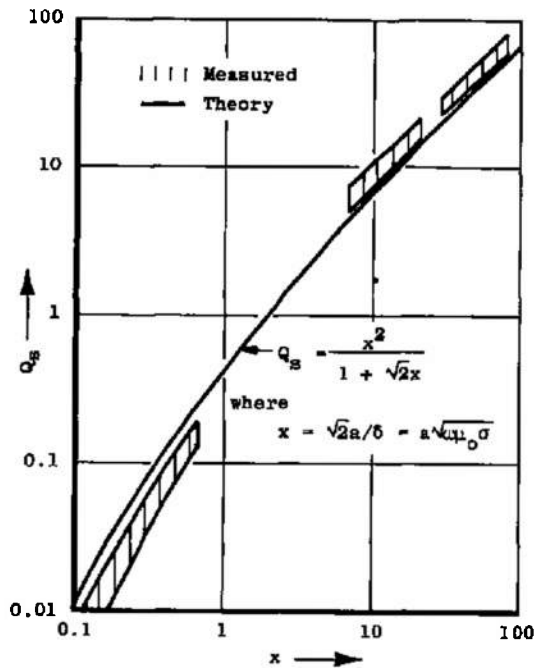


Fig. 3 Experimental and Theoretical Data for the Figure of Merit  $Q_s$  for a Solenoid Immersed in a Plasma

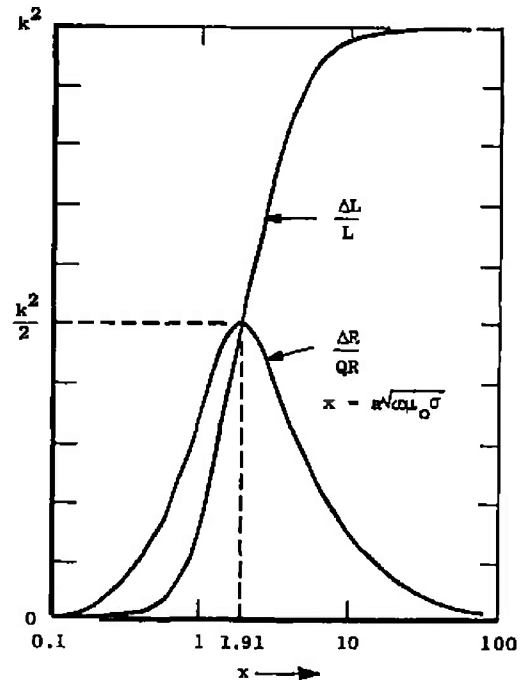


Fig. 4 Plot of  $\Delta L/L$  and  $\Delta R/QR$  versus  $x$  for a Solenoid Immersed in a Plasma

$k^2 L$  as the conductivity is further increased. In contrast, the change in coil resistance rises from zero for zero conductivity to a maximum value (at  $x = 1.91$ ) and then decreases toward zero as the conductivity is further increased. From this analysis, it is observed that the coil is most sensitive to the surrounding plasma when  $x$  is approximately equal to two. Thus, for a given range of plasma conductivities, an rf probe can be optimized for measurements in this range by proper selection of the frequency of excitation and the probe radius. That is,  $x$  is a function of  $\omega$  and  $a$  (external variables) and  $\sigma$  (an internal variable).

### 3.4 CALCULATION OF COIL PARAMETERS WHEN THE PLASMA IS IN THE INTERIOR OF THE SOLENOID

The coil-plasma configuration to be treated in this section is illustrated in Fig. 5. In this case, the plasma is located in the core of the coil.<sup>2</sup> Unlike the preceding example,

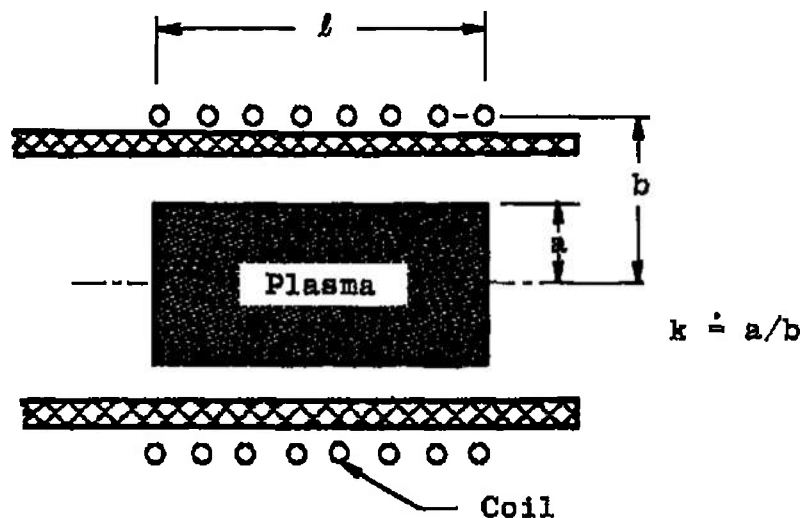


Fig. 5 Two-Dimensional View of Solenoid with a Plasma Core

the electric and magnetic fields are more readily obtained from an exact form of Maxwell's equation rather than by introducing an approximate expression for the gradient operator. Thus, if it is assumed that (1) the fields vary predominately in the radial coordinate, (2) the magnetic and electric fields are of the approximate forms, respectively,  $\vec{B}_c = \hat{i}_z B_z(\rho) \exp[j\omega t]$  and  $\vec{E}_c = \hat{i}_\phi E_\phi(\rho) \exp[j\omega t]$ , and (3)  $E_c$  is zero along the  $z$ -axis, then the magnetic and electric fields which satisfy Maxwell's equations in the region  $0 \leq \rho \leq a$  and  $-l/2 \leq z \leq l/2$  are<sup>3</sup>

$$B_c = \hat{i}_z B_a \left[ \frac{\text{ber } \gamma \rho + j \text{bei } \gamma \rho}{\text{ber } \gamma a + j \text{bei } \gamma a} \right] \exp[j\omega t] \quad (33)$$

<sup>2</sup>Although this form is used sometimes as a conductivity transducer, it is most often found in conjunction with rf plasma generation.

<sup>3</sup>The development of these solutions from Maxwell's equations is presented in Appendix II.

and

$$\vec{E}_c = \hat{i}_\phi \frac{\gamma B_a}{\sqrt{2} \mu_0 \sigma} \left[ \frac{(\text{ber}_1 \gamma \rho + \text{bei}_1 \gamma \rho) + (\text{bei}_1 \gamma \rho - \text{ber}_1 \gamma \rho)}{\text{ber } \gamma a + j \text{ bei } \gamma a} \right] \quad (34)$$

where  $B_a$  is the value of the magnetic field at  $\rho = a$ ,  $\gamma = \sqrt{\omega \mu_0 \sigma}$ , and ber and bei are Kelvin functions (Ref. 11).

The magnetic field in Eq. (33) is the field in the region ( $0 \leq \rho \leq a$ ), which results from both the eddy-currents ( $i_s$ ) and the primary current ( $i_p$ ). That is,

$$\vec{B}_c = \vec{B}_s + \vec{B}_p \quad (35)$$

where  $\vec{B}_s$  is the magnetic field due only to the eddy-currents in the plasma and  $\vec{B}_p$  is the magnetic field due only to the current in the coil.<sup>4</sup> It is important to be aware of this when calculating the figure of merit  $Q_s$  since, in this calculation, only the fields associated with the eddy-currents can be used in calculating energy stored and energy losses. The magnetic field inside a long solenoid located in free space is simply

$$\vec{B}_p = \hat{i}_z B_a \exp[j\omega t] \quad (36)$$

Thus, the field due to the eddy-currents alone is obtained by substituting Eqs. (33) and (36) into Eq. (35) and solving for  $B_s$ . That is,

$$\vec{B}_s = \hat{i}_z B_a \left[ \frac{(\text{ber } \gamma \rho - \text{ber } \gamma a) + j (\text{bei } \gamma \rho - \text{bei } \gamma a)}{\text{ber } \gamma a + j \text{ bei } \gamma a} \right] \exp[j\omega t] \quad (37)$$

The time-averaged energy stored ( $W_s$ ) is

$$\overline{W}_s = \frac{1}{2} \int_{-\ell/2}^{\ell/2} \int_0^{2\pi} \int_0^a \left( \frac{B_s \cdot B_s^*}{2\mu_0} + \epsilon \frac{E_c \cdot E_c^*}{2} \right) \rho d\rho d\phi dz \quad (38)$$

However, when  $\sigma \gg \omega\epsilon$ , then  $\frac{B_s \cdot B_s^*}{\mu_0} \gg \epsilon E \cdot E_s^*$ ; thus Eq. (38) reduces to

$$\overline{W}_s = \frac{\pi \ell B_a^2 \int_0^a \rho [(\text{ber } \gamma \rho - \text{ber } \gamma a)^2 + (\text{bei } \gamma \rho - \text{bei } \gamma a)^2] d\rho}{2\mu_0 [\text{ber}^2 \gamma a + \text{bei}^2 \gamma a]} \quad (39)$$

or after integration

$$\overline{W}_s = \frac{\omega \pi \ell B_a^2 a^2}{2\sqrt{2} \mu_0} \left[ \frac{(\text{ber } x + \text{bei } x) \text{ber}_1 x - (\text{ber } x - \text{bei } x) \text{bei}_1 x + \frac{x}{\sqrt{2}} (\text{ber}^2 x + \text{bei}^2 x)}{x[\text{ber}^2 x + \text{bei}^2 x]} \right] \quad (40)$$

<sup>4</sup>It is this type of separation of fields and currents in which the development of a transformer model for a coil-plasma system becomes apparent from a field viewpoint.

The energy loss per cycle ( $W_d$ ) is

$$W_d = \left( \frac{2\pi}{\omega} \right) \frac{1}{2} \int_{-\ell/2}^{\ell/2} \int_0^{2\pi} \int_0^a \sigma E_c \cdot E_c^* \rho d\rho d\phi dz = \left( \frac{2\pi}{\omega} \right) I_s^2 R_s \quad (41)$$

Substituting for  $E_c$  from Eq. (34) and integrating yield,

$$W_d = \left( \frac{2\pi}{\omega} \right) \left( \frac{\omega \pi \ell B_s^2 a^2}{\sqrt{2} \mu_0} \right) \left[ \frac{(\text{ber } x + \text{bei } x) \text{bei}_1 x + (\text{ber } x - \text{bei } x) \text{ber}_1 x}{x[\text{ber}^2 x + \text{bei}^2 x]} \right] \quad (42)$$

Thus, the figure of merit  $Q_s$  of a plasma located in the center of a coil is

$$Q_s = \frac{(\text{ber } x + \text{bei } x) \text{ber}_1 x - (\text{ber } x - \text{bei } x) \text{bei}_1 x + \frac{x}{\sqrt{2}} (\text{ber}^2 x + \text{bei}^2 x)}{(\text{ber } x + \text{bei } x) \text{bei}_2 x + (\text{ber } x - \text{bei } x) \text{ber}_2 x} \quad (43)$$

Equation (43) is plotted in Fig. 6 along with some experimental data. From these data, it is shown that the theory agrees quite well with experimental data, which is indicative of the ease and reliability of predicting the behavior of solenoids in the presence of conductive media. Further, this close agreement between the experiments and theory (see Figs. 3 and 6) indicates that the assumptions used to simplify and obtain closed-form solutions to Maxwell's equations (e.g., infinitely long coil) can be used with confidence for the finite length coil immersed in a conductive medium.

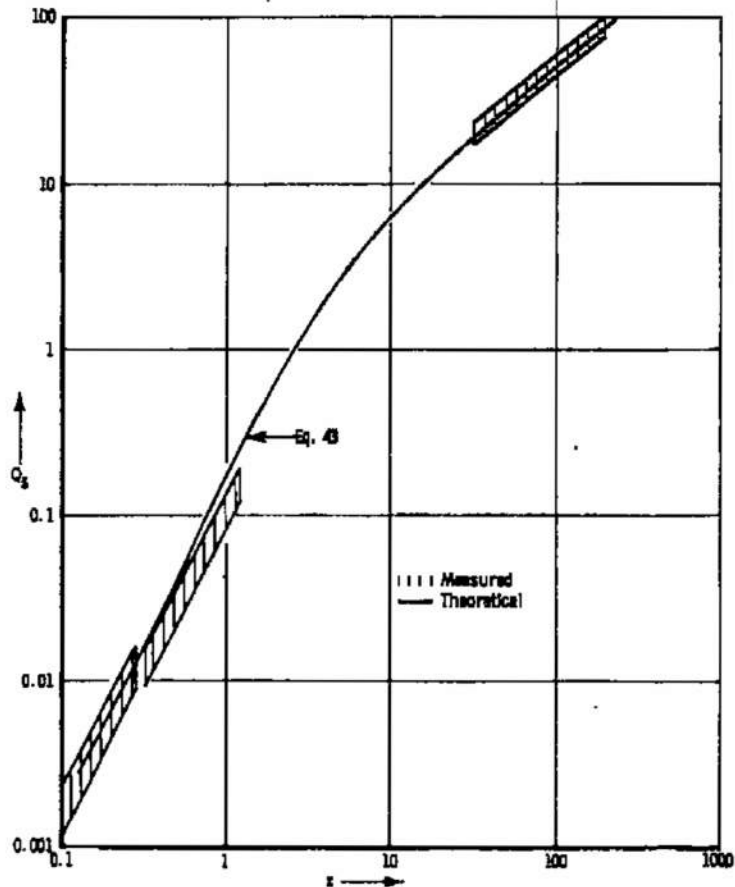


Fig. 6 Experimental and Theoretical Data for the Figure of Merit  $Q_s$  for Solenoid with a Plasma Core

## SECTION IV CONCLUDING REMARKS

Although the work reported herein has been concerned with cylindrically symmetric systems and with conductors with uniform conductivity, it should not be implied that this approach to the coupling problem is limited to these cases. The transformer model is equally valid for uniform and nonuniform conductors and also for other than cylindrically symmetric systems. If the system is more complex than outlined here, the difficulty will be in obtaining quantitative information since Maxwell's equation in this case will be much more difficult to solve.

The parameter  $Q_s$  has a fundamental definition in terms of energies and will still be a useful parameter to transform from circuit to field phenomena, even in the more complex systems. For example, it can be seen from Eq. (14) that the power input to the plasma is maximum when  $Q_s = 1$  regardless of the state of the plasma and the coil. Also from Fig. 4, it can be observed that the plasma behaves like a resistive element for lower values of  $Q_s$ , and for values of  $Q_s$  greater than or equal to ten, the plasma appears to be inductive. Thus, the value of  $Q_s$  for a plasma or other conductive media can be used to describe or predict the behavior of the plasma-coil system, and since  $Q_s$  is a function of the plasma diameter, frequency, and plasma conductivity, it is possible to adjust these parameters to match the desired test conditions.

It is recommended that  $Q_s$  be adopted as a correlating parameter in all rf experiments (either in plasma diagnostics or plasma generation) because (1) it is universal, (2) it encompasses and groups together the essential parameters of the plasma and coil, (3) it is nondimensional and thus does not depend on magnetic field strengths, currents, etc., and (4) it is readily expressed in terms of either circuit or field phenomena.

## REFERENCES

1. Stubbe, E.J. "An Absolute Immersion-Type Electrical Plasma Conductivity Probe." IEEE Proceedings, Vol. 56, pp. 1483-1493, September 1968.
2. Savic, P. and Boulton, G.T. "A Frequency Modulation Circuit for the Measurement of Gas Conductivity and Boundary Layer Thickness in a Shock Tube." National Research Council of Canada, MT43, May 1961.
3. Kawashima, N. "Plasma Density Measurements by Use of FM Demodulators." Japanese Journal of Appl. Phys., September 1964.
4. Dymshits, B.M. and Koretskii, Y.P. "An Experimental Investigation of Induced Discharges." Translated from Soviet-Physics-Technical Physics Vol. 9, pp. 1294-1298, 1965.
5. Eckert, H.U. "Analytical Solution of the Energy Balance Equation for Thermal Induction Plasmas in Argon." AIAA Paper No. 68-711, June 1968.

6. Johnston, P.D. "Temperature and Electron Density Measurements in an RF Discharge in Argon." *Physics-Letters*, Vol. 20, pp. 499-501, March 1966.
7. Sprouse, J.A. "Coupling Mechanism between Radio-Frequency Excited Coils and Conductive Media." UTSI M.S. Thesis, June 1967.
8. Sprouse, J.A. "Measurement of Electrical Conductivity in a Low-Density Supersonic Plasma." AEDC-TR-65-146 (AD473662), November 1965.
9. Keefer, D.R. "The Theory and the Diagnosis of the Electrodeless Discharge." University of Florida, Ph.D Thesis, August 1967.
10. Jackson, J.D. Classical Electrodynamics. John Wiley and Sons, Inc., New York, p. 238, 1962.
11. Handbook of Mathematical Functions. Applied Mathematics, Series 55. National Bureau of Standards, U.S. Government Printing Office, Washington, D.C. 1964.

## **APPENDIXES**

- I. PARALLEL-TUNED CIRCUIT AND MATCHING PROBLEMS**
- II. SOLUTION TO MAXWELL'S EQUATIONS FOR A CYLINDRICALLY SYMMETRIC SYSTEM**

## APPENDIX I PARALLEL-TUNED CIRCUIT AND MATCHING PROBLEMS

Generally, the rf-excited coil is the complementary part of a tuned circuit. This is true whether the coil is used as a source for intense electromagnetic fields required for electrodeless plasma generation or as a plasma diagnostic tool (e.g., conductivity transducer). Since the coil is often used in one arm of a resonant circuit and because impedance matching between the tuned circuit and the electronics is often a critical area on which proper operation of the system depends, then it becomes especially important to study this particular aspect of the plasma-coil relationship.

This appendix is concerned with the resonant system in which the coil is in parallel with a capacitor as indicated in Fig. I-1. The impedance  $Z'$  of the capacitor-inductor parallel circuit is

$$Z' = \frac{Q' \omega L' [1 + j \{Q' - \omega^2 L' C (Q'^2 + 1)/Q'\}] }{(Q'^2 + 1)(\omega^2 L' C)^2 + Q'^2 (1 - 2\omega^2 L' C)} \quad (\text{I-1})$$

The parallel circuit is said to be tuned (i.e., imaginary part of  $Z'$  is zero) when

$$C = \frac{1}{\omega^2 L'} \left( \frac{Q'^2}{Q'^2 + 1} \right) \quad (\text{I-2})$$

The real or resonant value of  $Z'_0$  is obtained by substituting Eq. (I-2) into Eq. (I-1). That is

$$Z'_0 = Q' \omega L' \left[ \frac{Q'^2 + 1}{Q'^2} \right] \quad (\text{I-3})$$

If  $Q'$  and  $L'$  in Eq. (I-1) are expressed in terms of the free-space coil parameters  $L$  and  $Q$

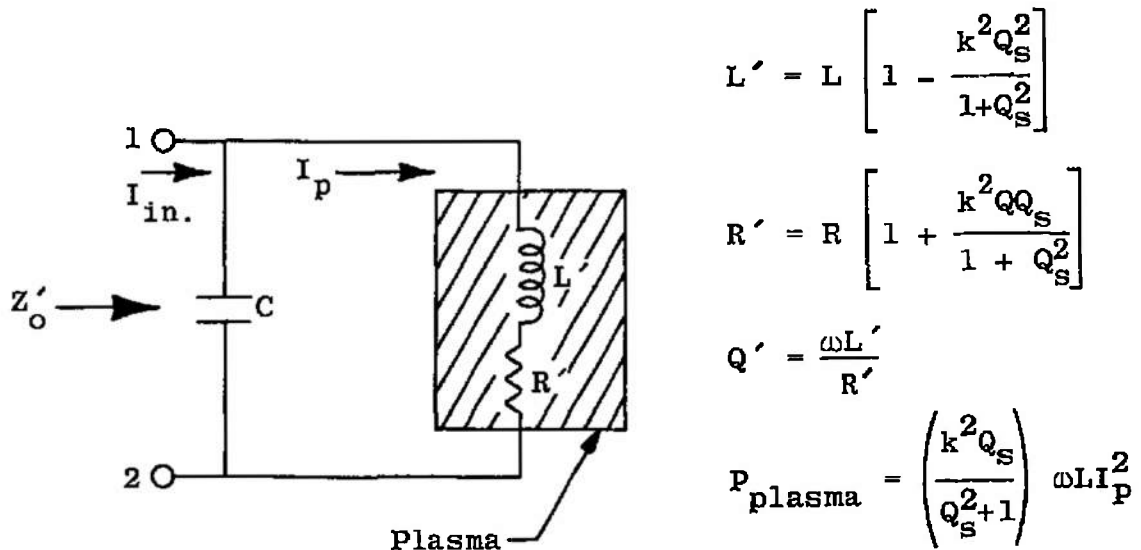


Fig. I-1 Parallel-Tuned Circuit with the Coil in the Presence of a Plasma



and in terms of the parameters  $k$  and  $Q_s$  by using the transformer model (see Fig. I-1), then  $Z'_o$  can be written as

$$Z'_o = Z_o f(k, Q_s) \quad (I-4)$$

where

$$Z_o = Q\omega L \quad (I-5)$$

and

$$f(k, Q_s) = \frac{Q_s^2 (1 - 2k^2 + k^4) + 2k^2 Q_s / Q + 1}{Q_s^2 + k^2 Q Q_s + 1} \quad (I-6)$$

The expression for  $Z'_o$  is plotted in Fig. I-2 for various values of the coupling coefficient  $k$  and for a free-space coil  $Q$  of 100. It can be seen from examination of Eq. (I-4) and Fig. I-2 that the impedance of the parallel-tuned circuit at resonance contains terms which depend on the physical characteristics of the coil (e.g., free-space inductance, free-space  $Q$ , and the coupling coefficient  $k$ ) as well as the parameter  $Q_s$ , which is functionally related to the physical and electrical characteristics of the plasma. Since the proper operation of the entire system (i.e., the electronics-coil-plasma complex) depends quite strongly on "matching phenomena," it is important to examine this aspect in some detail. It should be emphasized too that this electronics-coil-plasma complex is a coupled system and that optimization of the system demands that all aspects of matching be considered as a whole rather than independently. For instance, it is possible that an arrangement which might constitute an optimum match between the coil and plasma would create an unfavorable matching relationship between the electronics and coil which could result in an overall decrease in performance of the system.

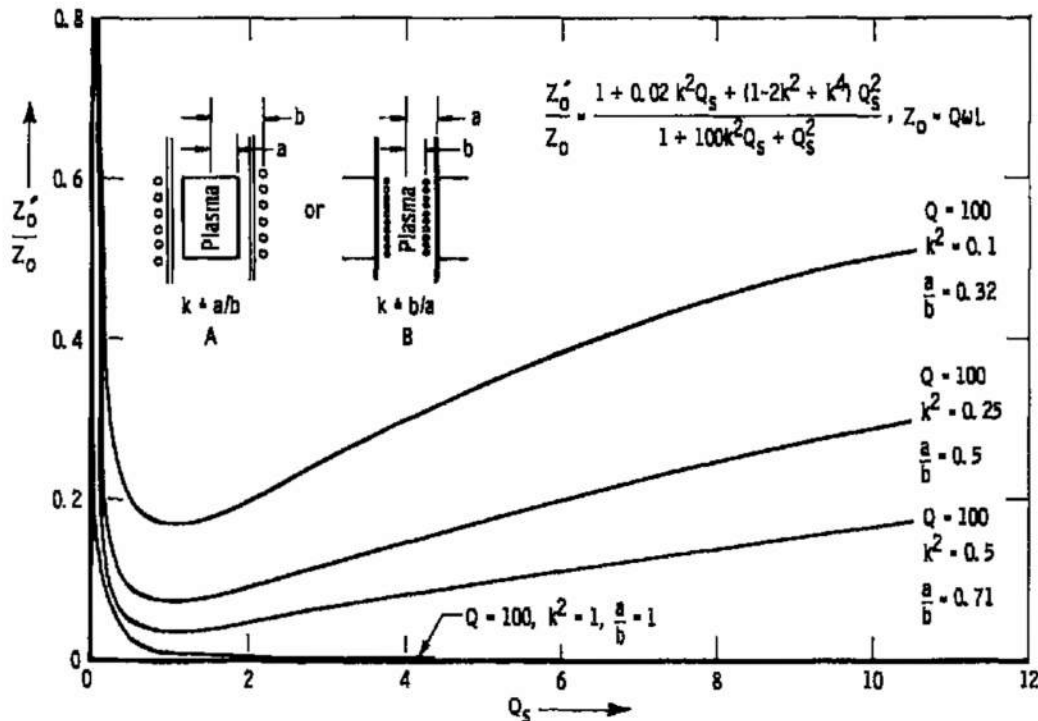


Fig. I-2 Plot of Normalized Impedance Ratio  $Z'_o/Z_o$  versus  $Q_s$

There is a specific area in which this aspect of the problem often creates confusion between various investigators of electrodeless discharges. This can be illustrated by considering the impedance  $Z'_o$  and the power input to the plasma from a system like that shown in Fig. I-1. The input to the plasma is

$$P_{\text{plasma}} = \omega L I_p^2 \left( \frac{k^2 Q_s}{Q_s^2 + 1} \right) \quad (\text{I-7})$$

From this expression, it is clear that maximum input power to the plasma is obtained when  $k = 1$  (actually the coupling coefficient must always be less than unity) and when  $Q_s = 1$ . That is,

$$(P_{\text{plasma}})_{\text{max}} = \frac{\omega L I_p^2}{2} \quad (\text{I-8})$$

Thus it appears from this analysis that the coil should be closely coupled to the plasma (i.e., the ratio of plasma to coil diameter should approach unity) if it is desirable to maximize the power input to the plasma for a given current  $I_p$ . (In practice, a mismatch generally results in a reduction in  $I_p$ .) However, when  $k$  and  $Q_s$  approach unity, the impedance  $Z'_o$  can drop from its free-space value  $Z_o$  by as much as two orders of magnitude (see Fig. I-2). This can have very serious consequences on the operation of the generator which supplies the rf power to the load, and it may happen that this value of impedance is much too low for coil-electronics matching.

Since the Class C oscillator is most often used for rf power generation, it is not a simple matter to determine the most favorable value of the load  $Z'_o$  a priori. The efficiency of operation is closely linked with the value of the load, and experimentally it is generally observed that values of  $Z'_o$  ranging from 1000 to 10,000 ohms are required for proper matching.

The point to be emphasized here is that the overall matching problem must be viewed in order to arrive at the proper rf system. Sometimes in rf plasma discharges, system performance has been improved by decreasing the coupling between the plasma and the coil. In cases like this, the explanation is that the impedance match between the coil and the generator was not satisfactory, and by decreasing the coupling between the coil and the plasma, the impedance of the tuned circuit was increased, which created a more favorable matching condition and improved system performance.

## APPENDIX II

### SOLUTION TO MAXWELL'S EQUATIONS FOR A CYLINDRICALLY SYMMETRIC SYSTEM

The coordinate nomenclature which is used in this report is shown in Fig. II-1.

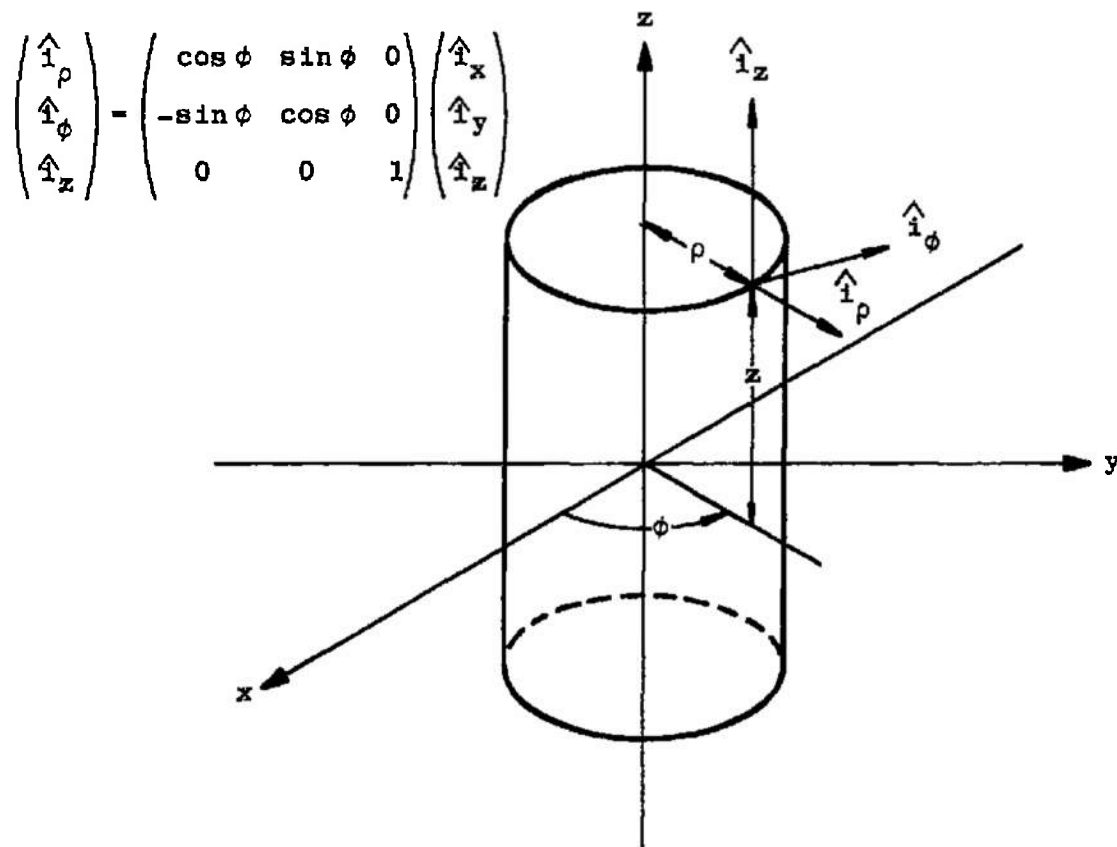


Fig. II-1 Diagram Illustrating Cylindrical Coordinates  $(\rho, \phi, z)$  and Unit Vectors  $(\hat{i}_\rho, \hat{i}_\phi, \hat{i}_z)$  with Respect to Cartesian Coordinates

The curl of a vector  $A$  in cylindrical coordinates is

$$\vec{\nabla} \times A = \frac{1}{\rho} \begin{bmatrix} \hat{i}_\rho & \rho \hat{i}_\phi & \hat{i}_z \\ \frac{\partial}{\partial \rho} & \frac{\partial}{\partial \phi} & \frac{\partial}{\partial z} \\ A_\rho & \rho A_\phi & A_z \end{bmatrix} \quad (\text{II-1})$$

Maxwell's equations are

$$\overrightarrow{\nabla \times E} = - \frac{\partial \overrightarrow{B}}{\partial t} \quad (\text{II-2})$$

$$\overrightarrow{\nabla \times B} = \mu_0 \overrightarrow{J} + \mu_0 \frac{\partial \overrightarrow{D}}{\partial t} \quad (\text{II-3})$$

$$\nabla \cdot B = 0 \quad (\text{II-4})$$

and

$$\nabla \cdot E = q/\epsilon \quad (\text{II-5})$$

When, (1) the electric and magnetic fields have a simple sinusoidal time variation (i.e.,  $e^{j\omega t}$ ), (2) the system is neutral (i.e.,  $q = 0$ ), (3) the constitutive equations are applicable (i.e.,  $\overrightarrow{J} = \sigma \overrightarrow{E}$  and  $\overrightarrow{D} = \epsilon \overrightarrow{E}$ ), and (4) the conduction current is much greater than the displacement current (i.e.,  $\sigma \gg \omega \epsilon$ ), then Maxwell's equations reduce to

$$\overrightarrow{\nabla \times E} = -j\omega \overrightarrow{B} \quad (\text{II-6})$$

$$\overrightarrow{\nabla \times B} = \mu_0 \sigma \overrightarrow{E} \quad (\text{II-7})$$

$$\nabla \cdot B = 0 \quad (\text{II-8})$$

and

$$\nabla \cdot E = 0 \quad (\text{II-9})$$

If it is assumed that the electric and magnetic fields are of the form

$$\overrightarrow{E} = \hat{i}_\phi E_\phi(\rho) e^{j\omega t} \quad (\text{II-10})$$

and

$$\overrightarrow{B} = \hat{i}_z B_z(\rho) e^{j\omega t} \quad (\text{II-11})$$

then the partial derivative ( $\partial/\partial \rho$ ) in Eq. (II-1) can be replaced by the total derivative ( $d/d\rho$ ). Thus, Eqs. (II-6) and (II-7) become, respectively,

$$\overrightarrow{\nabla \times E} = \hat{i}_z \left[ \frac{dE_\phi}{d\rho} + \frac{E_\phi}{\rho} \right] = -\hat{i}_z [j\omega B_z] \quad (\text{II-12})$$

and

$$\overrightarrow{\nabla \times B} = \hat{i}_\phi \frac{dB_z}{d\rho} = \hat{i}_\phi \mu_0 \sigma E_\phi \quad (\text{II-13})$$

or

$$E_\phi = - \frac{1}{\mu_0 \sigma} \frac{dB_z}{d\rho} \quad (\text{II-14})$$

Likewise

$$\frac{dE_\phi}{d\rho} = - \frac{1}{\mu_0 \sigma} \frac{d^2 B_z}{d\rho^2} \quad (\text{II-15})$$

An equation which contains only the magnetic field  $B_z$  can be obtained by substituting Eqs. (II-4) and (II-15) into Eq. (II-12). That is,

$$\frac{d^2 B_z}{d\rho^2} + \frac{1}{\rho} \frac{dB_z}{d\rho} - j\omega\mu_0\sigma B_z = 0 \quad (\text{II-16})$$

This equation can be transformed into Bessel's equation if the substitution  $z = \rho e^{-\pi j/4} \sqrt{\omega\mu_0\sigma}$  is made. That is, Eq. (II-16) becomes

$$z^2 \frac{d^2 B_z}{dz^2} + z \frac{dB_z}{dz} + z^2 B_z = 0 \quad (\text{II-17})$$

The general solution to Eq. (II-17) is

$$B_z = A J_0(z) + C Y_0(z) \quad (\text{II-18})$$

where  $J_0(z)$  and  $Y_0(z)$  are Bessel functions of the first kind and second kind, respectively, both of zero order. For a system in which  $B_z$  must be finite at the origin (i.e.,  $\rho = 0$ ) and has a value  $B_z = B_a$  at  $\rho = a$ , then Eq. (II-18) becomes

$$B_z = B_a \left[ \frac{J_0(e^{-\pi j/4} \sqrt{\omega\mu_0\sigma} \rho)}{J_0(e^{-\pi j/4} \sqrt{\omega\mu_0\sigma} a)} \right] \quad (\text{II-19})$$

The solution to Maxwell's equation for the electric field is obtained from Eqs. (II-14) and (II-19). That is,

$$E_\phi = -\frac{1}{\mu_0\sigma} \frac{dB_z}{d\rho} = e^{-\pi j/4} \sqrt{\frac{\omega}{\mu_0\sigma}} B_a \left[ \frac{J_1(e^{-\pi j/4} \sqrt{\omega\mu_0\sigma} \rho)}{J_0(e^{-\pi j/4} \sqrt{\omega\mu_0\sigma} a)} \right] \quad (\text{II-20})$$

Often it is more convenient to work with functions with real arguments. This can be done in the case of  $B_z$  and  $E_\phi$  in Eqs. (II-19) and (II-20) by using the following equation of transformation:

$$J_n(e^{-\pi j/4} v) = e^{-n\pi j} [\text{ber}_n v + j \text{bei}_n v] \quad (\text{II-21})$$

where  $n$  is the order and  $v$  is the argument. Thus, Eq. (II-19) becomes

$$B_z = B_a \left[ \frac{\text{ber}_0(\sqrt{\omega\mu_0\sigma} \rho) + j \text{bei}_0(\sqrt{\omega\mu_0\sigma} \rho)}{\text{ber}_0(\sqrt{\omega\mu_0\sigma} a) + j \text{bei}_0(\sqrt{\omega\mu_0\sigma} a)} \right] \quad (\text{II-22})$$

and Eq. (II-20) becomes

$$E_\phi = e^{\pi j/4} \sqrt{\frac{\omega}{\mu_0\sigma}} B_a \left[ \frac{\text{ber}_1(\sqrt{\omega\mu_0\sigma} \rho) + j \text{bei}_1(\sqrt{\omega\mu_0\sigma} \rho)}{\text{ber}_0(\sqrt{\omega\mu_0\sigma} a) + j \text{bei}_0(\sqrt{\omega\mu_0\sigma} a)} \right] \quad (\text{II-23})$$

## DOCUMENT CONTROL DATA - R &amp; D

(Security classification of title, body of abstract and indexing annotation must be entered when the overall report is classified)

1. ORIGINATING ACTIVITY (Corporate author) Arnold Engineering Development Center, ARO, Inc., Operating Contractor, Arnold Air Force Station, Tennessee 37389		2a. REPORT SECURITY CLASSIFICATION UNCLASSIFIED	
		2b. GROUP N/A	
3. REPORT TITLE  SOLENOIDS EXCITED AT RADIO-FREQUENCIES IN THE PRESENCE OF PLASMAS			
4. DESCRIPTIVE NOTES (Type of report and inclusive dates) September 1967 to December 1969 - Final Report			
5. AUTHOR(S) (First name, middle initial, last name)  J. A. Sprouse, ARO, Inc.			
6. REPORT DATE October 1970		7a. TOTAL NO. OF PAGES 29	7b. NO. OF REFS 11
8a. CONTRACT OR GRANT NO. F40600-71-C-0002		9a. ORIGINATOR'S REPORT NUMBER(S) AEDC-TR-70-206	
b. PROJECT NO. 8952-07			
c. Program Element 62201F		9b. OTHER REPORT NO(S) (Any other numbers that may be assigned this report) ARO-ETF-TR-70-184	
d.			
10. DISTRIBUTION STATEMENT  This document has been approved for public release and sale; its distribution is unlimited.			
11. SUPPLEMENTARY NOTES  Available in DDC.		12. SPONSORING MILITARY ACTIVITY Arnold Engineering Development Center (XON), Air Force Systems Command, Arnold AF Station, Tenn. 37389	

## 13. ABSTRACT

The rf-excited coil in the presence of a plasma is examined in terms of a transformer model and also in terms of the distortion of the electromagnetic fields which is produced by the induced eddy-currents in the plasma. The treatment of rf coils presented here can be applied to either the plasma diagnostics regime or to the generation of the rf electrodeless discharge. Although the calculations of the electric and magnetic fields in this report are for a cylindrically symmetric coil immersed in a uniform, linear plasma, neither the model nor the approach to the problem is limited to these cases.

14.

## KEY WORDS

## LINK A

## LINK B

## LINK C

ROLE

WT

ROLE

WT

ROLE

WT

plasma diagnostics  
solenoids  
electrodeless plasmas  
radio-frequency generators  
induction heating  
transformers  
electromagnetic fields